Electronic Supplementary Material (ESI) for Journal of Materials Chemistry A.

Supporting Information

Long-life Na-rich nickel hexacyanoferrate capable of working under stringent conditions

Yunpo Sun,[a] Yunli Xu,[b] Zheng Xu,[a] Yu Sun,[a] Xiongwen Xu,[c] Jian Tu,[c] Jian Xie,[*a] Shuangyu Liu[d] and Xinbing Zhao[a]

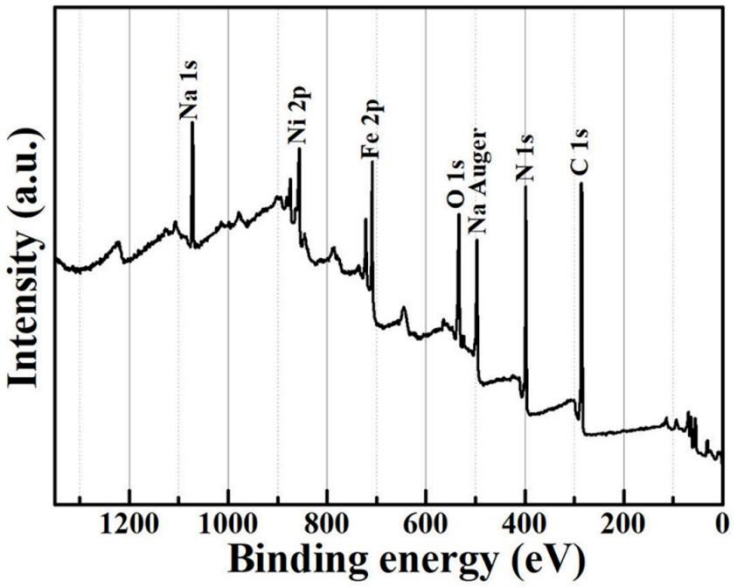

Fig. S1 XPS survey spectrum of NiHCF sample.

[a] *State Key Laboratory of Silicon Materials, School of Materials Science and Engineering, Zhejiang University, Hangzhou 310027, P. R. China. E-mail: xiejian1977@zju.edu.cn; Fax: +86-571-87951451; Tel: +86-571-87952181*
[b] *Zhejiang Research Institute of Product Quality and Safety, Hangzhou 310018, P. R. China*
[c] *LI-FUN Technology Corporation Limited, Zhuzhou 412000, P. R. China*
[d] *Zhejiang Huayun Information Technology Co., Ltd, Hangzhou 310008, P. R. China*

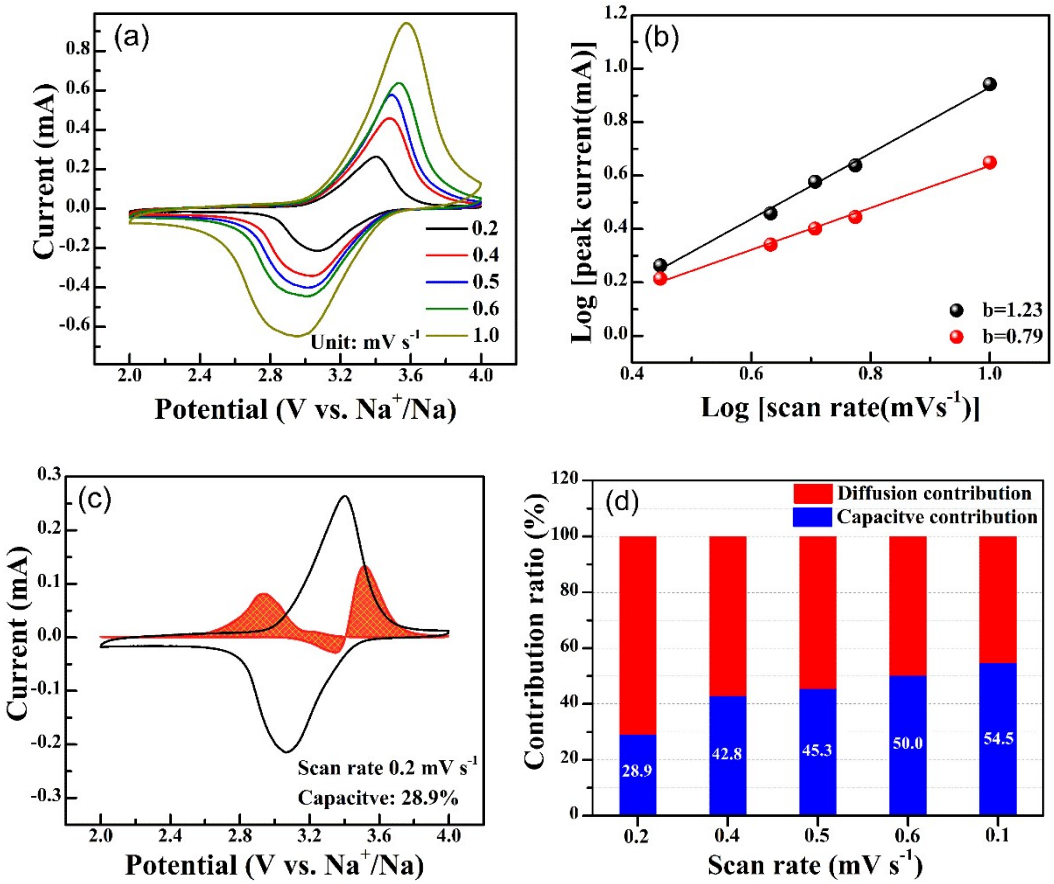

Fig. S2 (a) CV curves at various scan rate, (b) peak current at various scan rates, (c) capacitive contributions to Na storage scanned at 0.2 mV s^{-1} and (d) capacitive contributions at various scan rates of NiHCF.

CV scanning was conducted from 0.2 to 1 mV s^{-1}. The pseudocapacitive contribution can be obtained by equation: $i\,(V) = k_1 v + k_2 v^{0.5}$ using Bruce Dunn's method (Ref 57). Where i is the measured current, v is the scan rate, and $k_1 v$ and $k_2 v^{0.5}$ describe the surface-controlled and diffusion-controlled processes, respectively. The pseudocapacitive contribution at 0.2 mV s^{-1} is calculated to be 28.9%.

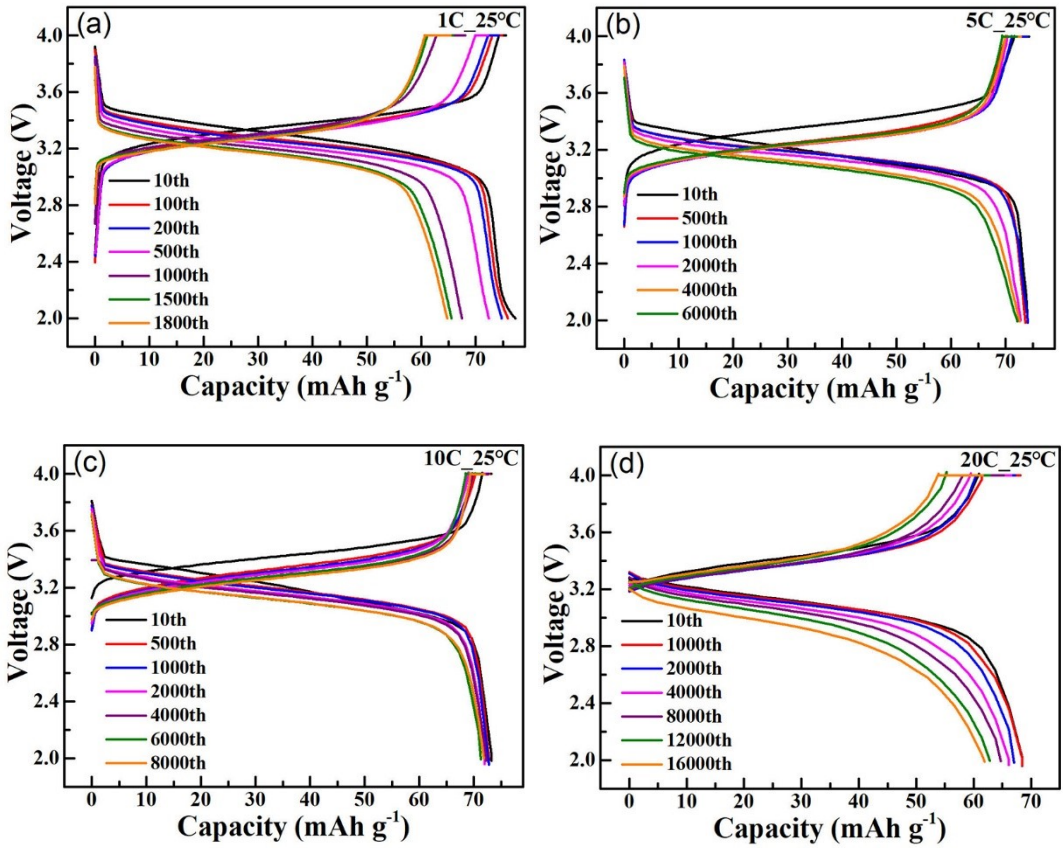

Fig. S3 Voltage profiles of NiHCF at 25°C at various discharge rates of (a) 1 C, (b) 5 C, (c) 10 C, and (d) 20 C.

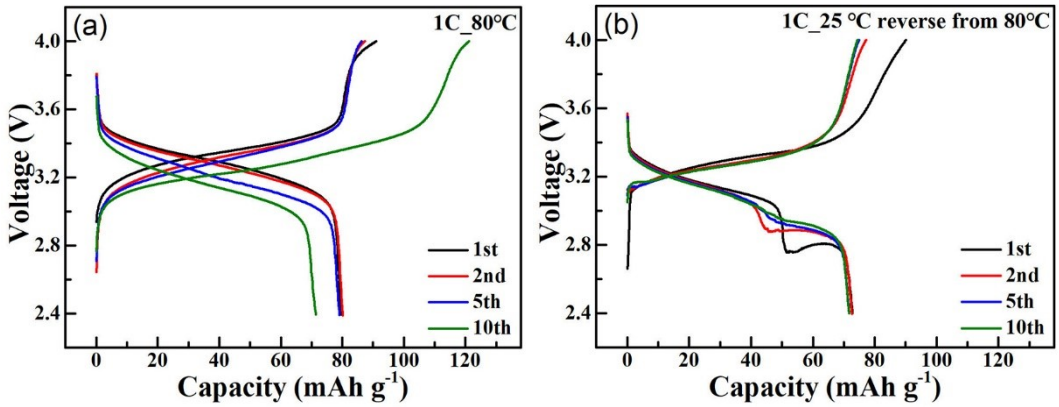

Fig. S4 (a) Voltage profiles at 80°C and (b) voltage profiles at 25°C after recovery from 80°C of NiHCF at 1 C.

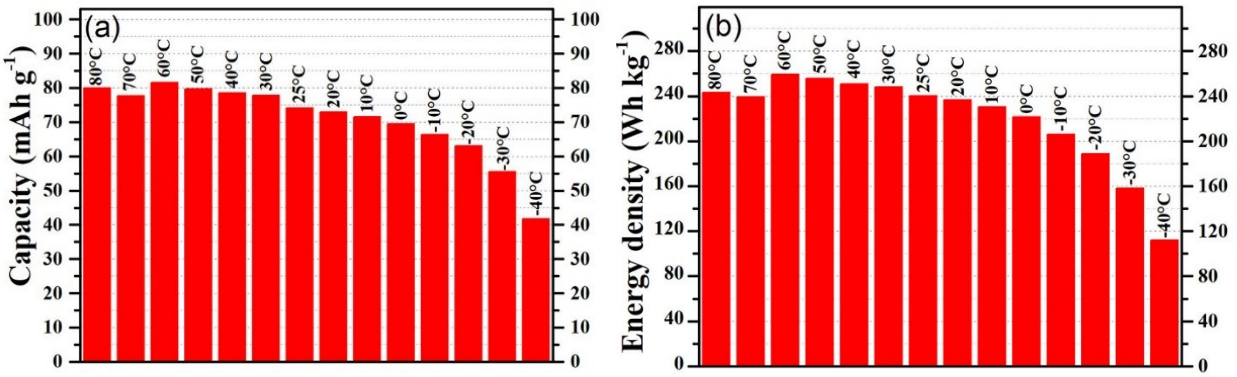

Fig. S5 Comparison of (a) discharge capacity and (b) energy density (based on NiHCF material only) at 1 C of NiHCF from –40°C to 80°C.

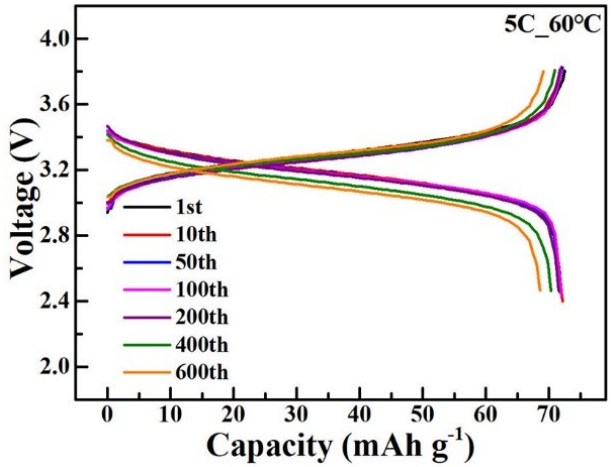

Fig. S6 Voltage profiles of NiHCF at 60°C cycled at 5 C.

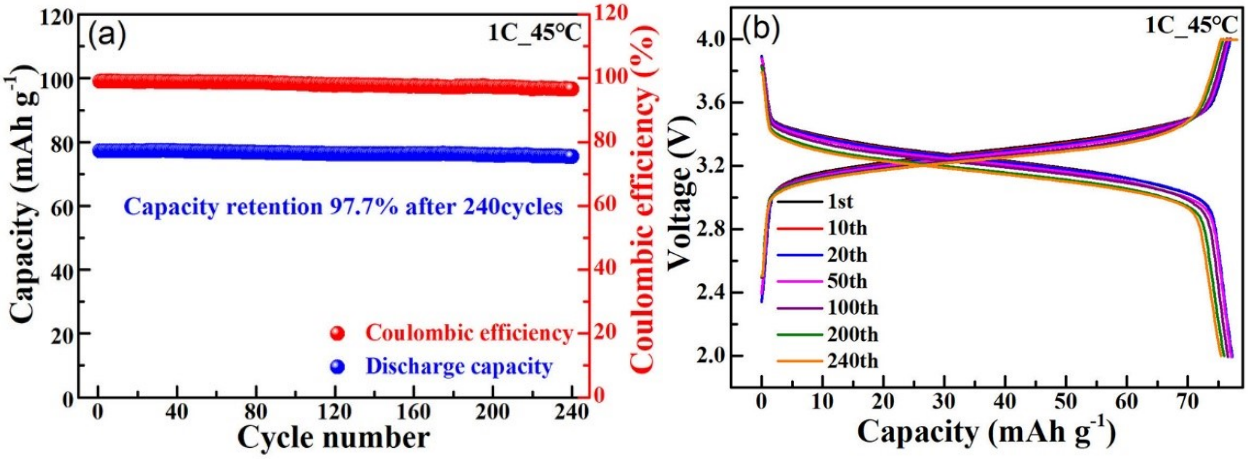

Fig. S7 (a) Cycling performance and (b) voltage profiles of NiHCF at 45°C at 1 C.

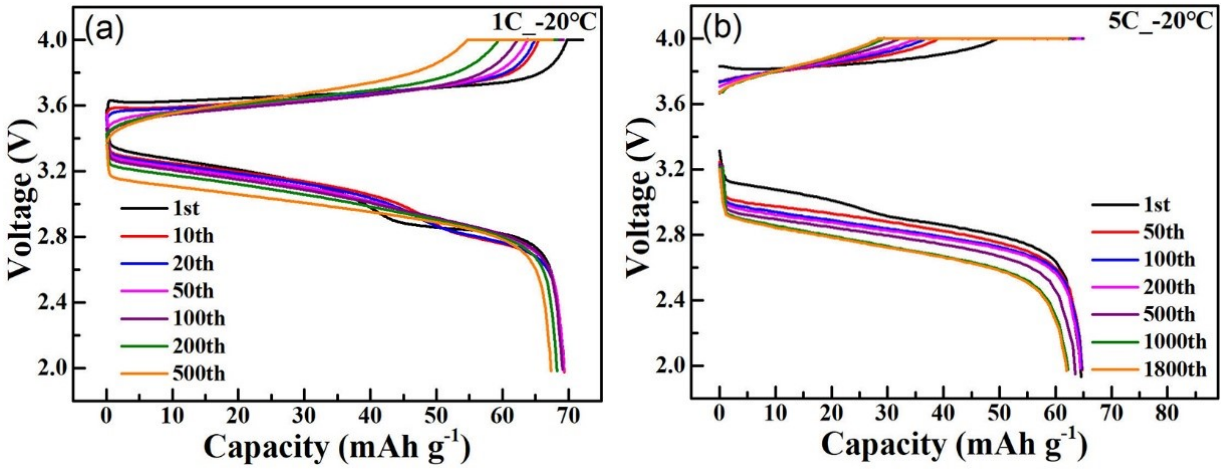

Fig. S8 Voltage profiles of NiHCF at –20°C cycled at (a) 1 C and (b) 5 C.

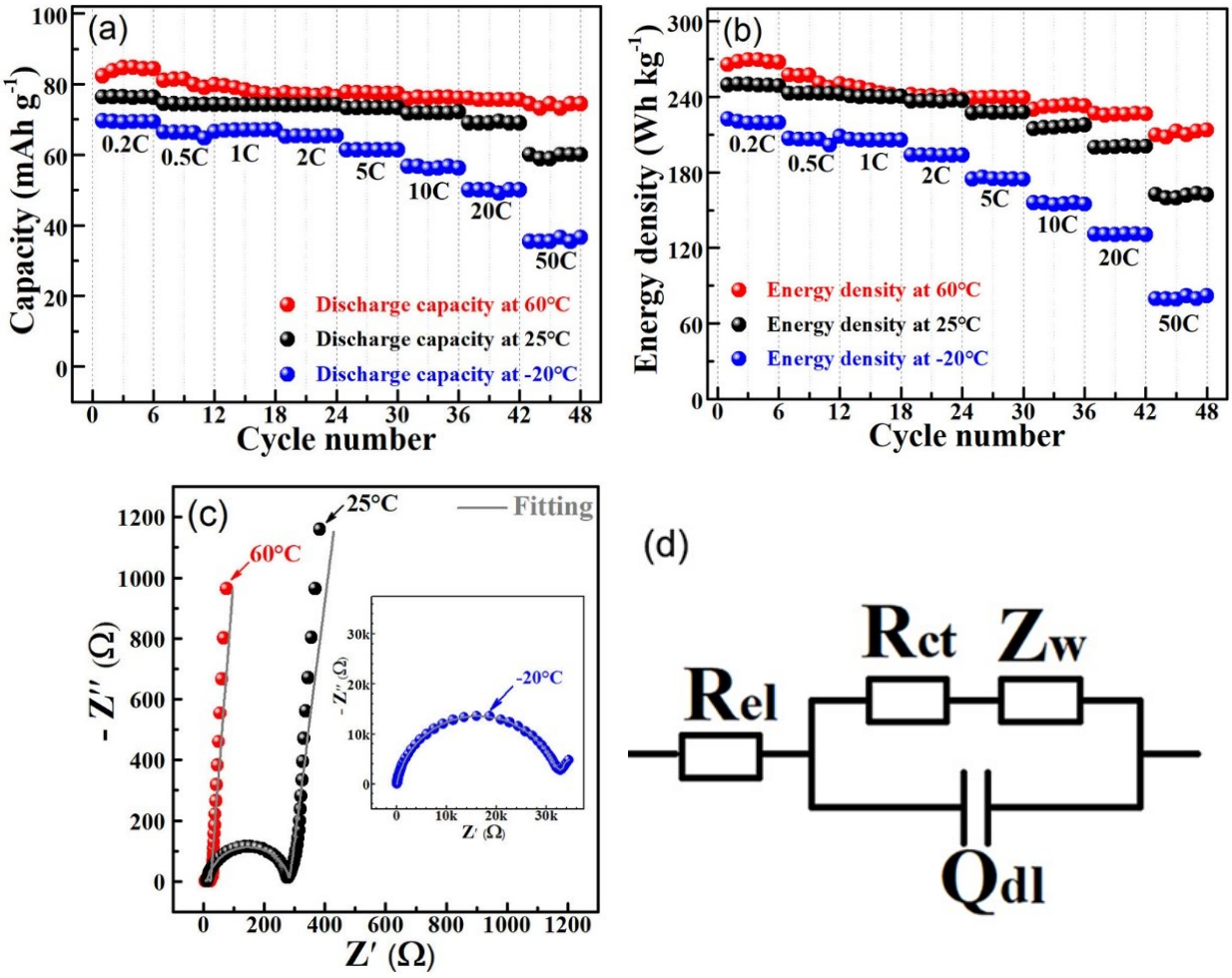

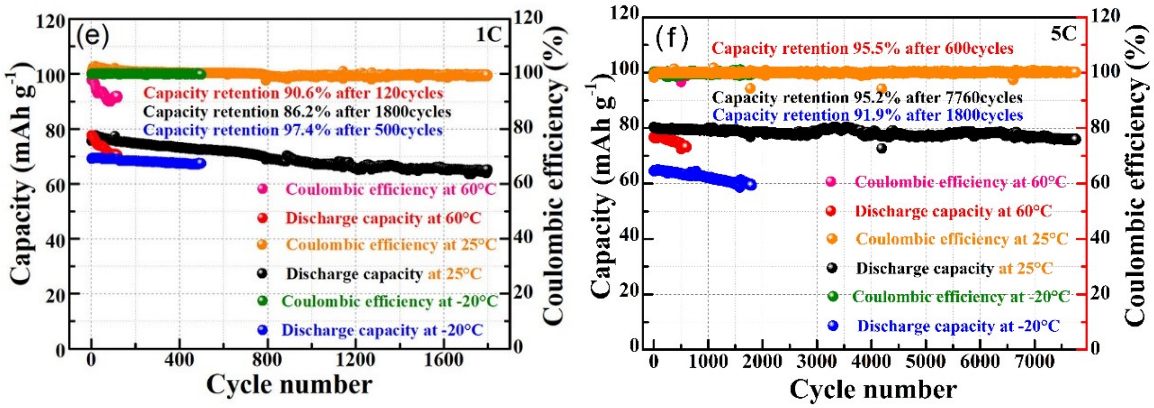

Fig. S9 Comparison of (a) rate capability, (b) energy density, and (c) EIS of NiHCF at 60°C, 25°C and –20°C, (d) equivalent circuit for EIS fitting, and comparison of cycling stability of NiHCF at 60°C, 25°C and –20°C at current rate of (e) 1 C and (f) 5 C.

To further understand the electrochemical behaviors of NiHCF, EIS measurements were performed at 60°C, 25°C and –20°C as shown in Fig. S9c. The impedance spectra are all composed of small semicircles in the high frequency region, which represents the charge transfer resistance (R_{ct}), and straight lines in the low frequency region, which corresponds to the Na^+ diffusion in the bulk material. The R_{ct} value at 25°C (272.2 Ω) and −20°C (32316 Ω) is higher than that at 60°C (15.2 Ω), indicating a temperature-sensitive charge transfer of the NiHCF. Although the R_{ct} is rather high at −20°C, the NiHCF material can still deliver acceptable capacity and rate performance, which may be due to rapid Na-ion diffusion in the open structure of the Prussian material.

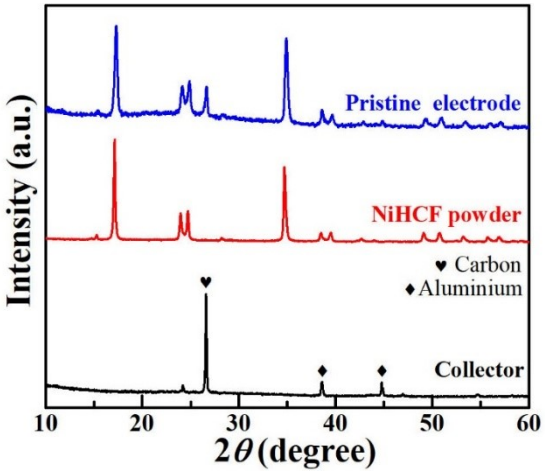

Fig. S10 XRD patterns of pristine NiHCF electrode, NiHCF powder, and Al current collector.

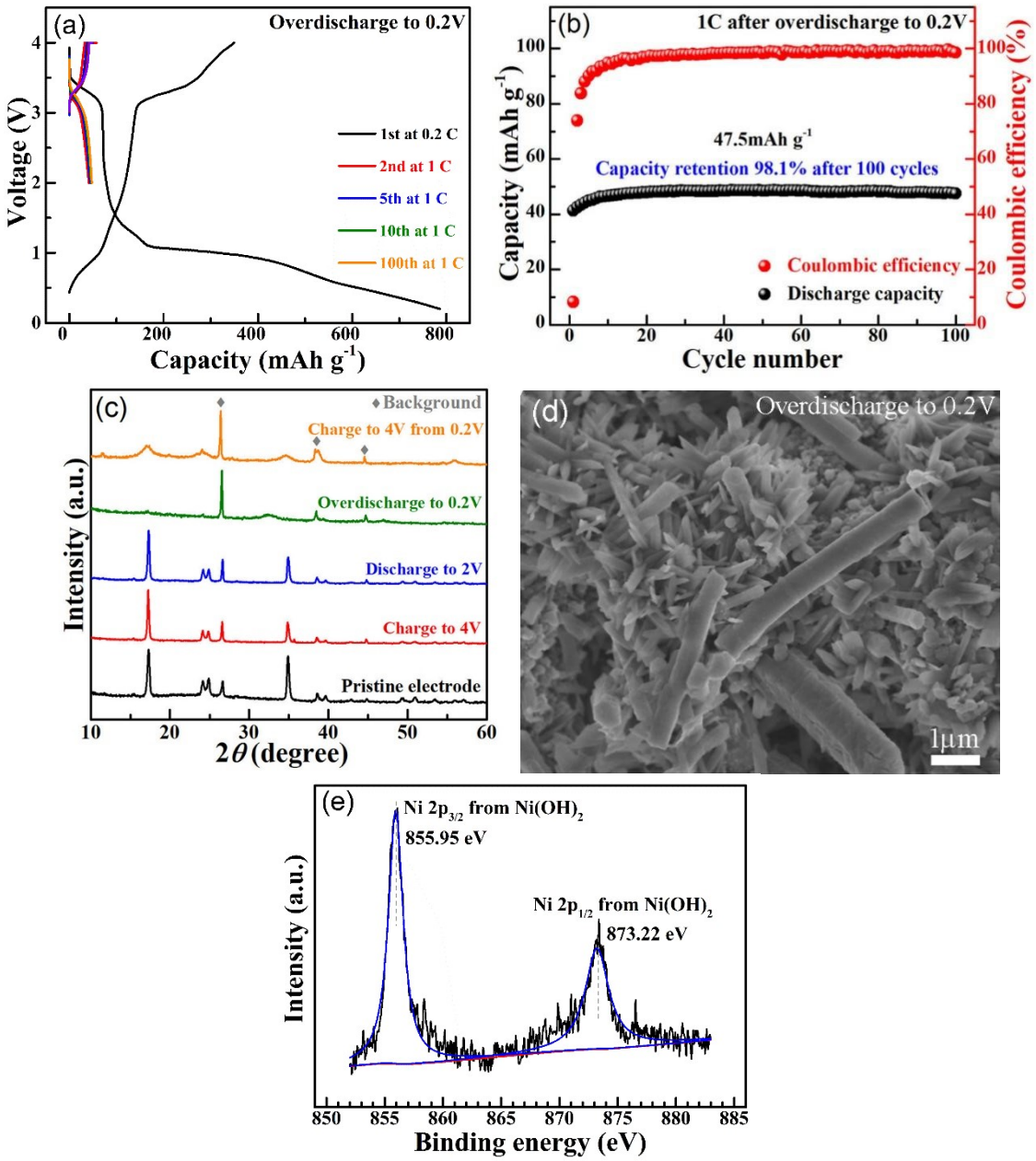

Fig. S11 (a) Overdischarge (to 0.2 V) tests of the NiHCF, (b) cycling stability of NiHCF at 1 C after overdischarge to 0.2 V, (c) XRD patterns of NiHCF electrodes at different charge/discharge states, and (d) SEM image and (e) Ni XPS spectrum of the NiHCF electrode after overdischarge to 0.2 V.

The deep overdischarge to 0.2 V leads to a high discharge capacity over 750 mAh g^{-1}. XRD and SEM indicate the complete crystal and morphology destruction of NiHCF as shown in Fig. S11c in Fig. S11d. XPS spectrum (Fig. S11e) confirms the breaking of the Ni–N bonds with the formation of $Ni(OH)_2$, which may be due to the oxidation of the metallic Ni (reduced from Ni^{2+} at deep overdischarge) by trace O_2 and H_2O in the electrolyte.

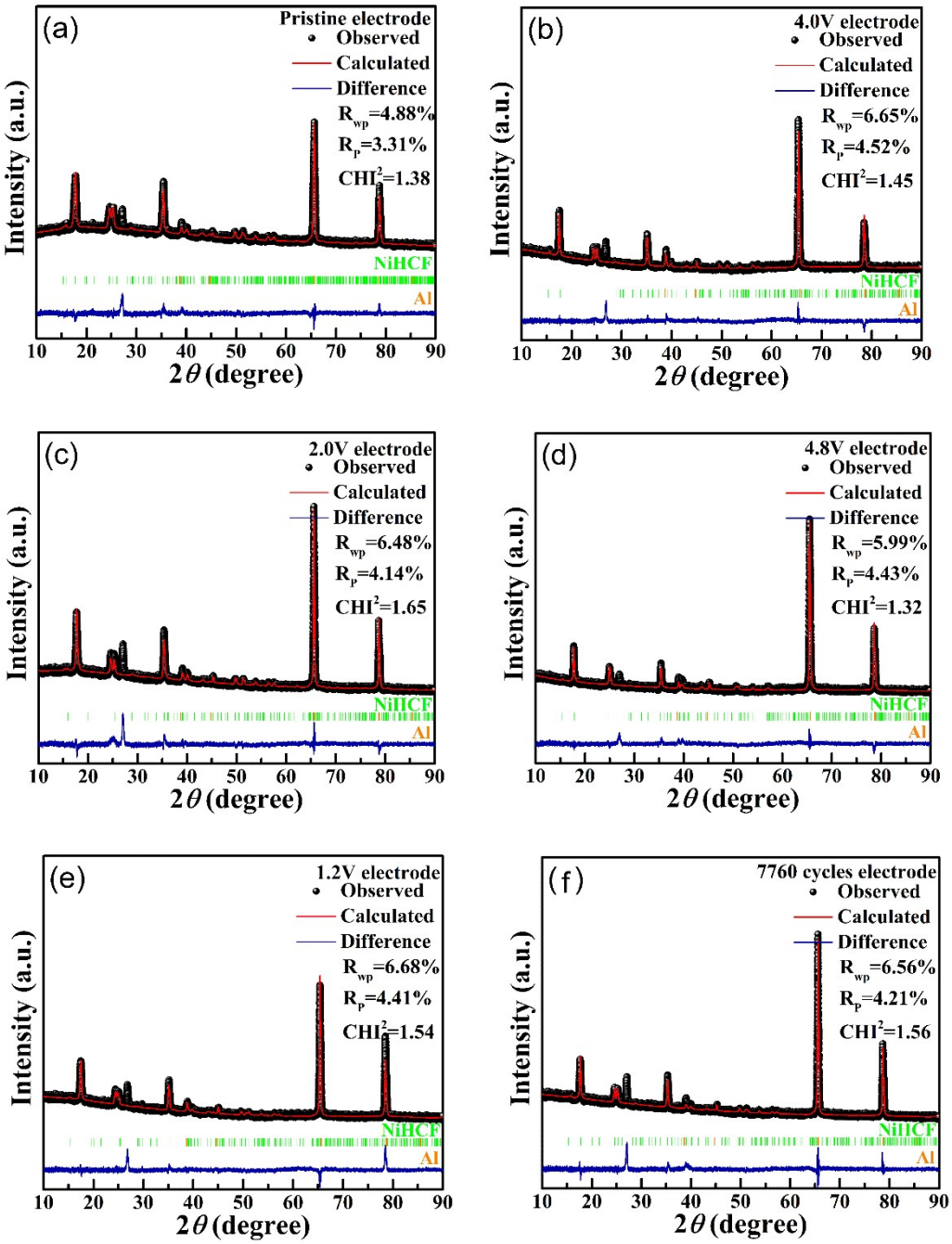

Fig. S12 Rietveld refinements of (a) pristine NiHCF electrode, (b) NiHCF electrode charged to 4.0 V, (c) NiHCF electrode discharged to 2.0 V, (d) NiHCF electrode overcharged to 4.8 V, (e) NiHCF electrode overdischarged to 1.2 V and (f) NiHCF electrode after 7760 cycles at 5 C at 25°C.

The Rietveld refinements of NiHCF electrode at various states are shown in Fig. S12. We give the lattice parameters from the Rietveld refinements for NiHCF electrodes in Table S7. The lattice parameters of NiHCF show minor changes after overcharge/overdischarge abuse. Even after 7760 cycles, lattice parameter only changes by 0.37%, implying a typical "zero strain" feature.

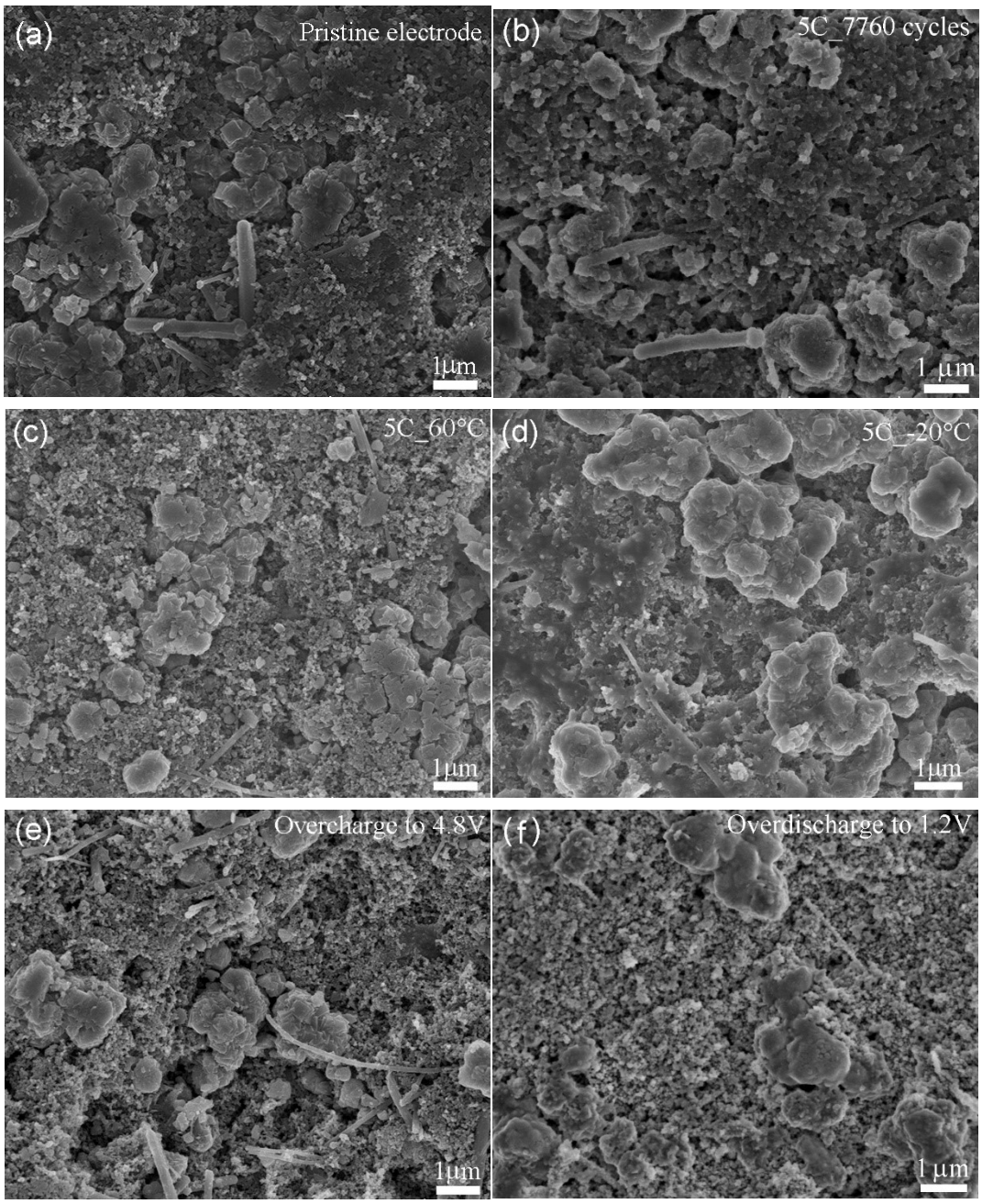

Fig. S13 SEM images of (a) pristine NiHCF electrode, (b) NiHCF electrode after 7760 cycles at 5 C at 25^{o}C, (c) NiHCF electrode after 500 cycles at 5 C at 60^{o}C, (d) NiHCF electrode after 500 cycles at 5 C at -20^{o}C, (e) NiHCF electrode after 500 cycles at 1 C after recovery from overcharge to 4.8 V, and (f) NiHCF electrode after 500 cycles at 1 C after recovery from overdischarge to 1.2 V.

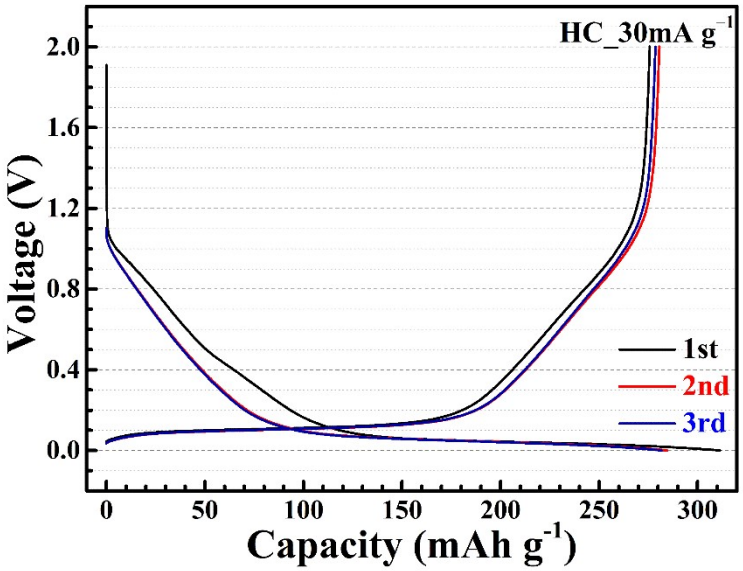

Fig. S14 Voltage profiles of hard carbon at 30 mA g^{-1}

The hard carbon demonstrates an operating voltage around 0.1 V, a reversible capacity about 275 mAh g^{-1}, and an initial coulombic efficiency close to 88%.

Information for Videos

Video 1: Synthesis of NiHCF using a 100 L reactor.

Video 2: The NiHCF/HC battery powers a toy car.

Table S1 Lattice parameters from the Rietveld refinements.

Lattice parameters of NiHCF	a / Å	b / Å	c / Å	α / °	β / °	γ / °	V / 10^6 pm^3
	7.167	7.396	12.301	90.000	123.283	90.000	545.133

Table S2 Atomic coordinates for Monoclinic NiHCF.

Atom	Wyck.	SOF	x	y	z	B / 10^4 pm^2
Ni1	2a	0.747277	0	0	0	2.921402
Fe	2d	0.813703	0.5	0	0.5	2.921402
C1	4e	0.539412	0.7041	0.319	0.0126	3.868883
C2	4e	0.769545	0.3232	0.0115	0.3131	3.868883
C3	4e	0.733218	0.3145	0.3152	0.004	3.868883
N1	4e	0.932472	0.8036	0.2031	0.0098	3.868883
N2	4e	0.931235	0.2117	0.0068	0.204	3.868883
N3	4e	0.829527	0.2059	0.2056	0.0031	3.868883
O1	4e	0.882312	0.0246	0.7252	0.261	3.868883
Na	4e	0.55	0.268	0.4554	0.2658	5.605933

Table S3 ICP results of NiHCF.

Elements	Tests	Weight (mg L^{-1})	Atom (mol mL^{-1})	Normalized
Na	1	3.356	0.146	2.224
	2	3.392	0.147	2.247
	3	3.319	0.144	2.199
Fe	1	2.892	0.052	0.789
	2	2.970	0.053	0.811
	3	3.000	0.054	0.819
Ni	1	3.902	0.066	1.013
	2	3.851	0.066	1.000
	3	3.903	0.067	1.014

Table S4 Electrochemical performance of NiHCF at 1 C from –40 to 80°C.

Temperature	Discharge capacity (mAh g^{-1})	Columbic efficiency (%)	Operate voltage (V)	Theoretical energy density (Wh kg^{-1})
80°C	80.1	48.93	3.11	243.2
70°C	77.8	82.20	3.12	239.5
60°C	81.6	97.41	3.22	259.5
50°C	79.8	98.32	3.24	256.0
40°C	78.5	98.61	3.22	250.9
30°C	77.8	99.02	3.22	248.1
25°C	74.2	99.88	3.27	240.3
20°C	72.9	99.91	3.29	236.8
10°C	71.6	99.93	3.27	230.7
0°C	69.6	99.96	3.23	221.8
-10°C	66.4	99.99	3.15	206.0
-20°C	63.1	100	3.04	188.8
-30°C	55.5	99.85	2.88	158.1
-40°C	41.8	99.56	2.71	112.0

Table S5 Rate capability of NiHCF at 25°C, 60°C and –20°C.

Temperature	Discharge rate	0.2 C	0.5 C	1 C	2 C	5 C	10 C	20 C	50 C
25°C	**Capacity (mAh g^{-1})**	76.4	74.4	74.2	74.2	73.3	71.9	69.1	59.7
	Capacity retention (%)	100.0	97.4	97.2	97.1	96.1	94.2	90.5	78.2
	Operation voltage (V)	3.32	3.3	3.27	3.23	3.13	3.06	2.96	2.79
	Voltage retention (%)	100.0	99.4	98.5	97.3	94.3	92.2	89.2	84.1
	Polarization voltage (V)	0	0.02	0.05	0.09	0.19	0.26	0.36	0.53
	Energy density (Wh kg^{-1})	249.5	242.9	240.3	236.9	227.8	216.2	200.4	161.6
	Energy retention (%)	100.0	97.4	96.3	94.9	91.3	86.7	80.3	64.8
60°C	**Capacity (mAh g^{-1})**	84.0	80.5	78.1	77.1	77.5	76.1	75.7	74.0
	Capacity retention (%)	110.1	105.4	102.4	100.9	101.6	99.8	99.2	97.0
	Operation voltage (V)	3.23	3.17	3.17	3.15	3.13	3.10	3.04	2.93
	Voltage retention (%)	97.3	95.5	95.4	95.0	94.2	93.3	91.7	88.4
	Polarization voltage (V)	0.09	0.15	0.15	0.17	0.19	0.22	0.28	0.39
	Energy density (Wh kg^{-1})	268.1	253.4	244.5	240.5	239.5	232.5	226.4	211.2
	Energy retention (%)	107.5	101.6	98.0	96.4	96.0	93.2	90.8	84.7
–20°C	**Capacity (mAh g^{-1})**	69.4	66.1	66.9	65.3	61.4	56.5	49.7	35.8
	Capacity retention (%)	90.9	86.6	87.7	85.6	80.4	74.0	65.1	46.9
	Operation voltage (V)	3.19	3.14	3.11	2.98	2.88	2.80	2.69	2.29
	Voltage retention (%)	96.1	94.5	93.7	89.9	86.7	84.4	81.0	69.0
	Polarization voltage (V)	0.13	0.18	0.21	0.34	0.44	0.52	0.63	1.03
	Energy density (Wh kg^{-1})	220.2	205.5	206.3	193.8	175.0	155.3	130.1	80.3
	Energy retention (%)	88.3	82.4	82.7	77.7	70.2	62.3	52.2	32.2

Notes: voltage retention is percentage of the operation voltage at 0.2 C at 25°C, polarization voltage is the difference with the operation voltage at 0.2 C at 25°C, energy density is the theoretical energy density for NiHCF material, and energy retention is percentage of the energy retention at 0.2 C at 25°C.

Table S6 EIS fitting results of NiHCF at different temperatures.

Sample	R_{el} / Ω	R_{ct} / Ω	Q_{dl}			W	
			Y	n	R	T	P
60°C	7.1	15.2	5.5×10^{-6}	0.91	3.2	0.033	0.48
25°C	11.8	272.2	6.1×10^{-6}	0.89	0.18	0.001	0.46
–20°C	73.5	32316	3.89×10^{-6}	0.89	14692	70.4	0.72

Table S7 Lattice parameters from the Rietveld refinements.

Lattice parameters	Pristine	Charged to 4 V	Discharged to 2 V	Charged to 4.8 V	Discharged to 1.2 V	7760 cycles
a / Å	7.1608	7.1920	7.1993	7.1786	7.2257	7.1798
b / Å	7.4144	7.3887	7.4175	7.3941	7.3134	7.4140
c / Å	12.3609	12.3512	12.3240	12.4642	12.5490	12.4115
α / °	90	90	90	90	90	90
β / °	123.2803	123.3346	123.4323	123.6694	124.8551	123.5396
γ / °	90	90	90	90	90	90
V / 10^6 pm^3	548.6416	548.3526	549.2198	550.6126	544.1820	550.6732
V difference /10^6 pm^3	0.0000	0.2890	0.5782	1.9710	4.4596	2.0316
Variance ratio	**0.00%**	**-0.05%**	**0.11%**	**0.36%**	**-0.81%**	**0.37%**

Table S8. Comparison of cycling performance of PBAs.

Material	Temperature (°C)	Current density (mA g^{-1})	Initial capacity (mAh g^{-1})	Cycle number	Final capacity (mAh g^{-1})	Capacity retention	Reference
NiHCF	**25**	**1700**	**68.5**	**16000**	61.9	**90.4%**	**This work**
NiHCF	**25**	**850**	**73.2**	**8000**	72.5	**99.1%**	**This work**
NiHCF-3	25	170	~76	800	68.4	90%	[1]
NiHCF-3	25	300	~76	1200	~75	99.5%	[2]
HQ-NiHCF	25	170	78	1200	76.4	98%	[3]
NiHCF-cube	25	495	~65	5000	50.0	76.9%	[4]
NiHCF-etch	25	495	~82	5000	68.2	83.2%	[4]
NiHCF	**25**	**425**	**73.8**	**6200**	72.2	**97.8%**	**This work**
NiHCF	**60**	**425**	**71.9**	**600**	68.7	**95.5%**	**This work**
NiHCF	**–20**	**425**	**64.6**	**1800**	59.4	**91.9%**	**This work**
PBNi-ES	25	85	82.7	440	72.0	87%	[5]
PBNi-ES	0	85	79.3	440	69.0	87%	[5]
PBNi-ES	–25	85	64.3	440	54.0	84%	[5]
PBFe/CNT	25	2.4C	114	1000	92.3	81%	[6]
PBFe/CNT	0	2.4C	114	1000	92.3	81%	[6]
PBFe/CNT	–25	2.4C	88.4	1000	76.0	86%	[6]
PBFe	55	100	120.5	200	65.9	54.7%	[7]
PBFe	25	100	100.0	300	98.2	98.2%	[7]
PBFe	–10	100	83.7	200	83.6	99.8%	[7]
NiHCF//Zn cell	**25**	**400**	**61.8**	**3100**	52.0	**84.1%**	**This work**
NiHCF//Zn cell	25	500	~56	1000	~45	81%	[8]
NiHCF//Zn cell	25	500	~68	1000	~61	91%	[9]

Table S9. Comparison of rate capability of NiHCF.

Material	Temperature (°C)	Current density (mA g^{-1})	Initial capacity (mAh g^{-1})	Cycle number	Final capacity (mAh g^{-1})	Capacity retention	Reference
NiHCF	**25**	**17**	**76.4**	**4250**	59.7	**78.2%**	**This work**
NiHCF	**60**	**17**	**84.0**	**4250**	74.0	**88.1%**	**This work**
NiHCF	**–20**	**17**	**69.4**	**4250**	35.8	**51.6%**	**This work**
NiHCF-3	25	17	86.3	**4250**	64.4	74.6%	[1]
NiHCF-3	25	17	85.7	**4250**	66.8	78.0%	[2]
HQ-NiHCF	25	15	80	750	62.0	77.5%	[3]
NiHCF- etch	25	100	90	4000	71.0	78.8%	[4]
PBNi-ES	25	8.5	80.3	2125	56.0	69.7%	[5]
PBNi-ES	0	42.5	74.0	425	58.5	79.1%	[5]
PBNi-ES	–25	42.5	62.0	425	16.3	26.3%	[5]
NiHCF//Zn cell	**25**	**16**	**69.0**	**4000**	41.0	**59.4%**	**This work**
NiHCF//Zn cell	25	100	~76	1000	~44.0	58%	[8]
NiHCF//Zn cell	25	100	84.8	4000	70.4	83%	[9]

References

1 Y. Xu, M. Chang, C. Fang, Y. Liu, Y. G. Qiu, M. Y. Ou, J. Peng, P. Wei, Z. Deng, S. X. Sun, X. P. Sun, Q. Li, J. T. Han and Y. H. Huang, *ACS Appl. Mater. Interfaces*, 2019, **11**, 29985–29992.

2 Y. Xu, J. Wan, L. Huang, M. Y. Ou, C. Y. Fan, P. Wei, J. Peng, Y. Liu, Y. G. Qiu, X. P. Sun, C. Fang, Q. Li, J. T. Han, Y. H. Huang, J. A. Alonso and Y. S. Zhao, *Adv. Energy Mater.*, 2019, **9**, 1803158.

3 R. Rehman, J. Peng, H. C. Yi, Y. Shen, J. W. Yin, C. Li, C. Fang, Q. Li and J. T. Han, *RSC Adv.*, 2020, **10**, 27033–27041.

4 W. H. Ren, M. S. Qin, Z. X. Zhu, M. Y. Yan, Q. Li, L. Zhang, D. N. Liu and L. Q. Mai, *Nano Lett.*, 2017, **17**, 4713–4718.

5 X. H. Ma, Y. Y. Wei, Y. D. Wu, J. Wang, W. Jia, J. H. Zhou, Z. F. Zi and J. M. Dai, *Electrochim. Acta*, 2019, **297**, 392–397.

6 Y. You, H. R. Yao, S. Xin, Y. X. Yin, T. T. Zuo, C. P. Yang, Y. G. Guo, Y. Cui, L. J. Wan and J. B. Goodenough, *Adv. Mater.*, 2016, **28**, 7243–7248.

7 X. M. Yan, Y. Yang, E. S. Liu, L. Q. Sun, H. Wang, X. Z. Liao, Y. S. He and Z. F. Ma, *Electrochim. Acta*, 2017, **225**, 235–242.

8 K. Lu, B. Song, J. T. Zhang and H. Y. Ma, *J. Power Sources*, 2016, **321**, 257–263.

9 F. X. Ma, X. H. Yuan, T. Xu, S. Y. Zhou, X. S. Xiong, Q. Zhou, N. F. Yu, J. L. Ye, Y. P. Wu and T. van Ree, *Energy Fuels*, 2020, **34**, 13104 − 13110.